



CO₂ hydrogenation reaction over pristine Fe, Co, Ni, Cu and Al₂O₃ supported Ru: Comparison and determination of the activation energies



Robin Mutschler^{*}, Emanuele Moioli, Wen Luo, Noris Gallandat, Andreas Züttel^{*}

Laboratory of Materials for Renewable Energy (LMER), Institute of Chemical Sciences and Engineering (ISIC), Basic Science Faculty (SB), École polytechnique fédérale de Lausanne (EPFL) Valais/Wallis, Energypolis, Rue de l'Industrie 17, CP 440, CH-1951 Sion, Switzerland
Empa Materials Science & Technology, CH-8600 Dübendorf, Switzerland

ARTICLE INFO

Article history:

Received 5 July 2018

Revised 31 July 2018

Accepted 1 August 2018

Available online 22 August 2018

Keywords:

CO₂

Hydrogenation

Activation energy

Pristine metals

Reaction thermodynamics

Reaction kinetics

ABSTRACT

Fe, Co, Ni and Cu are the main non-noble industrially significant catalysts in the CO₂ and CO gas phase hydrogenation reaction towards hydrocarbons and alcohols. These catalysts are typically supported on metal oxides such as SiO₂, TiO₂, Al₂O₃ and ZnO, in order to maximize the activity towards the desired reaction. The role of the supporting material is to stabilize the catalytic nanoparticles and to prevent sintering at the elevated reaction temperatures and pressures. The supporting phase can improve the reaction activity or even have a crucial role in the reaction, as is the case, e.g. for the Methanol synthesis over Cu based catalysts supported on ZnO. Studying the metals without a supporting oxide phase is of great importance for the fundamental understanding of the catalytic activity of the metal phase. Therefore, we investigated the pristine transition metals Fe, Co, Ni and Cu (diluted with silica glass beads to avoid sintering) towards their activity in the CO₂ hydrogenation reaction and determined the activation energy. An Al₂O₃ supported Ruthenium catalyst with 0.5 mass percent of Ru loading was taken as reference system. It was found that Co, Ni and Ru/Al₂O₃ are mostly active in the Sabatier reaction, while Fe is active in the reverse water gas shift reaction. Cu as pristine metal shows no catalytic activity. C₂+ hydrocarbons were formed on Co in low concentrations. For the calculation of the activation energy, the kinetically determined temperature range of the reaction is identified with a high resolution in time by means of a quantitative gas analysis method with an online mass spectrometer. The observation activation energy of the CO₂ hydrogenation reaction was determined to be 50 kJ/mol over Fe, 77 kJ/mol over Co, 74 kJ/mol over Ni and 73 kJ/mol over the Ru/Al₂O₃ catalyst. This indicates similar reaction pathways over Co, Ni and Ru/Al₂O₃ and a different reaction mechanism on Fe.

© 2018 Elsevier Inc. All rights reserved.

1. Introduction

Energy storage is crucial for the development of an energy supply based on renewable energy. The energy supply from wind -and solar power plants is intermittent in time due the day/night cycles, weather conditions, and seasonality. Since the supply of electricity must correspond to the demand in the power grid at all times to keep the grid frequency stable, energy storage is required to buffer the fluctuations from the stochastically producing energy converters such as wind- and solar power plants. Batteries are favorable for efficient short term storage, but are too costly to provide

long-term storage capacity [1]. Liquid synthetic fuels are a promising energy carrier for seasonal energy storage due to their high gravimetric -and volumetric energy density and stability in ambient conditions which is up to a hundred times larger than in batteries [2,3]. CO₂ extracted from air can be hydrogenated with hydrogen produced by electrolysis driven by renewable energy. The energy is then stored in the chemical bond of the hydrocarbons and is released upon combustion which is net CO₂ emission free. Today's technologies allow CO₂ hydrogenation via the reverse water gas shift reaction (RWGS) to CO, followed by the Fischer-Tropsch reaction (FTR) [4]. The FTR is an unselective reaction which leads to a wide hydrocarbon product distribution ranging from low molar weight gaseous hydrocarbons, alcohols and long chained waxes [5]. Therefore, energy intensive refining of the products is required to obtain a specific hydrocarbon fraction. The CO₂ hydrogenation via the Sabatier reaction is instead a selective reaction, with methane as the major product. Fe, Co, Ni, Cu, Ru and Rh

^{*} Corresponding authors at: Laboratory of Materials for Renewable Energy (LMER), Institute of Chemical Sciences and Engineering (ISIC), Basic Science Faculty (SB), École polytechnique fédérale de Lausanne (EPFL) Valais/Wallis, Energypolis, Rue de l'Industrie 17, CP 440, CH-1951 Sion, Switzerland.

E-mail addresses: robin.mutschler@epfl.ch (R. Mutschler), andreas.zuetzel@epfl.ch (A. Züttel).

are the most active elements known for the CO and CO₂ hydrogenation reaction and they are the key building blocks of the industrially significant catalysts [6,7]. In order to increase the surface area, the catalysts are typically nanosized particles supported on metal oxides such as Al₂O₃, SiO₂, TiO₂, ZnO and ZrO₂ to stabilize the active species, prevent sintering [8] and adapt the reaction selectivity [9]. In particular in the case of Cu, the support phase has a principal role in the CO₂ hydrogenation reaction mechanism [6,10]. The metal-support interactions and the influence on the reaction's activity and selectivity are not fully understood yet and a full understanding of these phenomena is crucial for the design of new, more selective catalysts. Therefore, it is of great interest to investigate the direct CO₂ hydrogenation over the unsupported pristine metal catalysts. This has been done on single crystal catalysts in Ultrahigh Vacuum (UHV) conditions [11,12] and by means of density functional theory calculations (DFT) [13–15] and micro kinetic reaction modeling [16,17]. The CO₂ hydrogenation reaction on Fe, Co, Ni and Cu catalyst on different supports – and also in their pristine form, was the object of numerous studies in the 1970s after the interest in synthetic fuels increased due to the oil crisis [18–20]. Nevertheless, a direct comparison of the pristine metal catalysts in similar reaction conditions with the determination of the activation energy has not been reported so far.

In this paper the activity of the pristine transition metals Fe, Co, Ni and Cu for the CO₂ hydrogenation reaction is investigated. The reaction was carried out in a micro reactor in quasi equilibrium conditions, meaning that the space velocity (around 1000 h⁻¹) and heating rate (1 K/min) were relatively low. For the product gas composition analysis, a quantitative gas analysis method by means of mass spectrometry (MS) has been developed, allowing the determination of the product gas stream composition, and therefore the calculation of the kinetic parameters, with a high resolution in time. The catalyst activity results are discussed in the frame of a thermodynamic reaction analysis.

2. Experimental

The experiments were carried out in a stainless-steel plug flow reactor placed in a tubular furnace. Three thermocouples are placed in – or on the reactor in order to monitor the reaction temperature. The temperature measured in the reaction tube in close vicinity to the catalyst bed is used as reference temperature for the reaction. The gas flows were controlled via three mass flow controllers for CO₂, H₂ and He. The gas lines after the reactor to the analysis instruments were heated to 200 °C to avoid condensation of products and water.

The gas stream has been analyzed by means of a Mass Spectrometer (Pfeiffer OmniStar 320) with a Faraday and Secondary Electron Detector (MS-SEM) and a Gas Chromatograph (SRI 8610C) equipped with a Flame Ionization Detector (FID) and a Thermal Conductivity Detector (TCD).

For the gas analysis, a software application was developed within MATLAB R2016b for the GC and MS to quantify the partial pressures in the product gas stream as a function of the reaction temperature.

The metal powders of Fe, Co, Ni and Cu were obtained from Goodfellow (Table SI) and examined for their purity by means of X-ray photoelectron spectroscopy (XPS). No impurities were detected by means of XPS. The catalysts were reduced with Hydrogen at elevated temperatures prior to the experiment to obtain a purely metallic surface. The specific weight of the catalyst and the surface area of the catalysts used in this study were determined by means of SEM (to estimate the particle size) and liquid N₂ adsorption isotherms to determine the specific surface area.

Supplementary data associated with this article can be found, in the online version, at <https://doi.org/10.1016/j.jcat.2018.08.002>.

2.1. Catalyst preparation and packing

In preliminary experiments, it was found that the metal powders can sinter during the reaction at elevated temperatures up to 650 °C. In particular, Co and Cu powders are prone to sinter. This caused clogging of the reactor, making the experiment not reproducible. Since it was the aim not to alter the reaction with a supporting phase, the catalyst powders were pressed to 8 mm pellets with a weight equivalent of four tons and then broken down to smaller grains with an approximate diameter of 1–1.5 mm. The grains were then mixed in an equal weight ratio with glass beads in the same size regime to prevent grain agglomeration. The glass beads are made of borosilicate glass and were purchased at Schäfer Glas. They have a diameter of 1 mm and were not affected by the reaction conditions. With this preparation method of the catalyst, no macroscopic sintering effects were observed after the experiments, thus enabling comparable reaction conditions among the four pristine metals.

2.2. Catalyst pretreatment with helium and hydrogen

To evaporate moisture from the catalyst and the tubing, the reactor and tubing were preheated with an applied He gas flow of 10 ml/min for a minimum time of 30 min. The reactor was preheated to 150 °C, the tubing to 200 °C. Subsequently, the catalysts were reduced with H₂ to obtain a metallic surface. This was done with a H₂ flow of 7.5 ml/min and 2.5 ml/min of He at a starting temperature of 150 °C. The temperature was then ramped up with 10 °C/min to a set point of 700 °C, while simultaneously measuring the gas composition with the MS. With this TPR, the temperature ranges at which the surface is reduced from oxides and carbides is determined via the formation of water (*m/z* 18 peak) and methane (*m/z* 16 peak). In case the surface reduction was not completed at the set point temperature after ramping up, the temperature was kept at the set point of 700 °C to further reduce the surface until the *m/z* 18 and *m/z* 16 peaks declined.

2.3. CO₂ hydrogenation experiment

After reducing the catalyst with H₂, the experimental gas flow was set with the gas stream going through the reactor bypass. The experimental gas flow was: CO₂ 1.5 ml/min, H₂ 6 ml/min and He 2.5 ml/min. Therefore, the total flow was 10 ml/min and the H₂:CO₂ ratio 4:1. The gas flow rate of 10 ml/min for the reaction gas stream was chosen as a tradeoff between quasi equilibrium conditions, MFC reliability (MFC models: Bronkhorst El Flow series. Flow range: 0.4–20 ml/min. Absolute measurement error in ml/min: 0.1% of maximum set point (20 ml/min) plus 0.5% of set point) and the time the gas product gas stream requires to reach the analysis systems (there is less than a minute of dead time between the reactor and the MS inlet at a flow of 10 ml/min). After the setpoint gas mixture was reached, the valve to the reactor was opened, the bypass closed, the temperature ramping set to 1 °C min and the measurement with MS and GC started. The maximum reactor oven temperature was set to 700 °C. The total time for the CO₂ hydrogenation experiment therefore takes 550 min since the ramping was started at 150 °C. The experiments were carried out in ambient pressure. The reactor is a plug flow reactor with a total length of 180 mm. The inner diameter of the reaction zone, which starts 75 mm after the inlet, is 7 mm in diameter (*d*_{i,2}). Before the reaction zone, the inner tube diameter is 4 mm (*d*_{i,1}). The catalyst is held in place to the inlet site by a sintered steel filter with a pore size of approximately 60 μm (Swagelok SS-2F-K4-60) and a diameter of 7 mm, which sits on a step of the inner tube at 75 mm from the inlet site. To load the catalyst, a small layer of glass wool is

inserted on top of the solid filter. Then, the catalyst is loaded and topped with another layer of glass wool to keep the catalyst in place to the outlet site. To calculate the space velocity, the distance l_{catalyst} between the first layer of glass wool and the top of the loaded catalyst is measured. The space velocity is then calculated as follows:

$$SV \left[\frac{1}{h} \right] = \frac{\dot{V}_{\text{reactants}} \left[\frac{\text{ml}}{h} \right]}{V_{\text{reactor}} \left[\text{ml} \right]} = \frac{\dot{V}_{\text{reactants}}}{\left(l_{\text{catalyst}} * \left(\frac{d_{i2}}{2} \right)^2 \pi \right)}$$

2.4. Data acquisition and analysis

The product gas stream was analyzed with the MS and GC. The MS has a sampling rate of approximately 2 min per scan, while the GC requires 17.5 min for measurement cycle. Since the heating rate was 1 °C/min (minimal setpoint possible at the oven), the temperature between two spectra is approximately 2 K for the MS and 17.5 K for the GC. The kinetically determined temperature ranges are typically around 30 K wide. Therefore, the GC has less than two data points for this range which is not sufficient to determine the kinetic reaction range with a heating ramp of 1 K/min. The accurate identification of the kinetic reaction range is the basis for the calculation of the activation energy. To enable the reaction to be carried out in one day, the heating ramp was not to be reduced. Therefore, a quantitative gas analysis by means of mass spectrometry was developed, where a fast data acquisition was achieved. The GC was used as backup instrument to the MS and to identify C2+ hydrocarbon products. Throughout this study, the Faraday detector and a scan width of 1–100 mass/charge (m/z) and a scan speed of 1 s per m/z was used for the MS. In the first step after the experiment, the spectra are loaded into an array in MATLAB R2016b, where they were correlated to the reaction temperature. Then the partial pressures of the gases were calculated based on the calibration spectra. Since the internal pressure of the MS can change over the course of the experiment, the signal intensity varies with this pressure change since a higher difference in pressure between the MS and the gas line means a higher gas flow into the MS and therefore a stronger signal. Since this does not influence the composition of the gas, the sum of all partial pressures of the detected species was normalized at the total reaction pressure in every measurement point. With that, the partial pressures of all detected gas species are known for every spectrum. The CO₂ conversion, product yield –and selectivity are calculated based on the principle of mass conservation with the carbon balance. Since methane and carbon monoxide are the only carbon containing reaction products of significant quantity, the CO₂ conversion is calculated based on the partial pressure of the reaction products p_{CH_4} , p_{CO} and the partial pressure of CO₂ after the reaction.

$$P_{\text{products}} = p_{\text{CH}_4} + p_{\text{CO}}$$

$$X_{\text{CO}_2} = \frac{P_{\text{products}}}{P_{\text{products}} + P_{\text{CO}_2, \text{out}}}$$

The yield of methane Y_{CH_4} is calculated as follows:

$$Y_{\text{CH}_4} = X_{\text{CO}_2} * \frac{P_{\text{CH}_4}}{P_{\text{products}}}$$

The carbon monoxide yield Y_{CO} is then given by:

$$Y_{\text{CO}} = X_{\text{CO}_2} - Y_{\text{CH}_4}$$

The selectivity S_i of each product i is given by:

$$S_i = \frac{P_i}{P_{\text{products}}}$$

The full derivation of the CO₂ conversion calculation is given in the supplementary information.

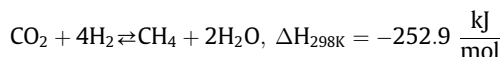
3. Results and discussion

3.1. Thermodynamics

The maximal conversion of CO₂ at a given pressure and temperature is defined by the thermodynamic equilibrium conversion at this working point. Thermodynamic limitations are independent from the catalyst. In this study, two products containing carbon were detected in significant quantities: CH₄ and CO. The observed reactions are the Sabatier and Reverse Water Gas Shift (RWGS) reactions. In the following, the thermodynamic equilibria for the two standalone reactions and for the simultaneous formation of CH₄ and CO as functions of temperature and pressure is given. In all, five gas species are present as reactants and products (CO, CO₂, H₂, H₂O and CH₄), and have to be taken into consideration in the equilibria calculations.

3.1.1. Equilibrium conversion to CH₄ and CO as function of pressure and temperature

The conversion of CO₂ to CH₄ is an exothermic reaction and the product formation is therefore favored at low reaction temperatures. Following the Le-Chatelier principle, an increase in reaction pressure shifts the equilibrium to the product side, since the overall number of moles is decreased during the reaction. Therefore, a higher reaction pressure increases the concentration of the product at thermodynamic equilibrium. The Sabatier reaction is given by:



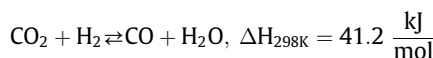
The thermodynamic equilibrium is calculated with the Van't Hoff equation and the equilibrium constant which is given by the partial reaction pressures. With the stoichiometry of the reaction, the equilibrium is expressed as function of the total reaction pressure and the partial pressure of CH₄.

$$-\frac{\Delta G_{\text{R}}(T)}{RT} = -\frac{\Delta H_{\text{R}}(T)}{RT} + \frac{\Delta S_{\text{R}}(T)}{R} = \ln(K_{\text{eq}})$$

With $K_{\text{eq,CH}_4}$ given by (assuming ideal gas behavior)

$$K_{\text{eq,CH}_4} = \frac{p_{\text{CH}_4} * p_{\text{H}_2\text{O}}^2}{p_{\text{CO}_2} * p_{\text{H}_2}^4} = \frac{p_{\text{CH}_4} * 4p_{\text{CH}_4}^2}{\left(\frac{4}{5}(p_{\text{tot}} - 3p_{\text{CH}_4}) * \frac{1}{5}(p_{\text{tot}} - 3p_{\text{CH}_4})\right)}$$

Similarly, the equilibrium constant for the RWGS is calculated independently of the Sabatier reaction. The RWGS reaction is given by:



$$K_{\text{eq,CO}} = \frac{p_{\text{CO}} * p_{\text{H}_2\text{O}}}{p_{\text{CO}_2} * p_{\text{H}_2}} = \frac{p_{\text{CO}}^2}{\left(\frac{1}{2}p_{\text{tot}} - p_{\text{CO}}\right)^2}$$

The equations for $K_{\text{eq,CH}_4}$ and $K_{\text{eq,CO}}$ are implicit since the reaction enthalpy and entropy are temperature dependent and the equation must be solved numerically. The parameters to calculate the temperature dependent reaction enthalpy and entropy are from the NIST chemistry WebBook. The calculated equilibria as function of temperature and at three different reaction pressures are presented in Fig. 1.

3.1.2. Simultaneous equilibrium conversion to CH₄ and CO

To have a thermodynamic foundation for the interplay between the Sabatier and the RWGS reaction, the equilibrium conversion taking into consideration both reactions, was calculated. The result is plotted in Fig. 2. The Sabatier reaction is dominant at low reaction temperatures up to approximately 800–900 K (depending also on the reaction pressures). The RWGS is only favored at higher

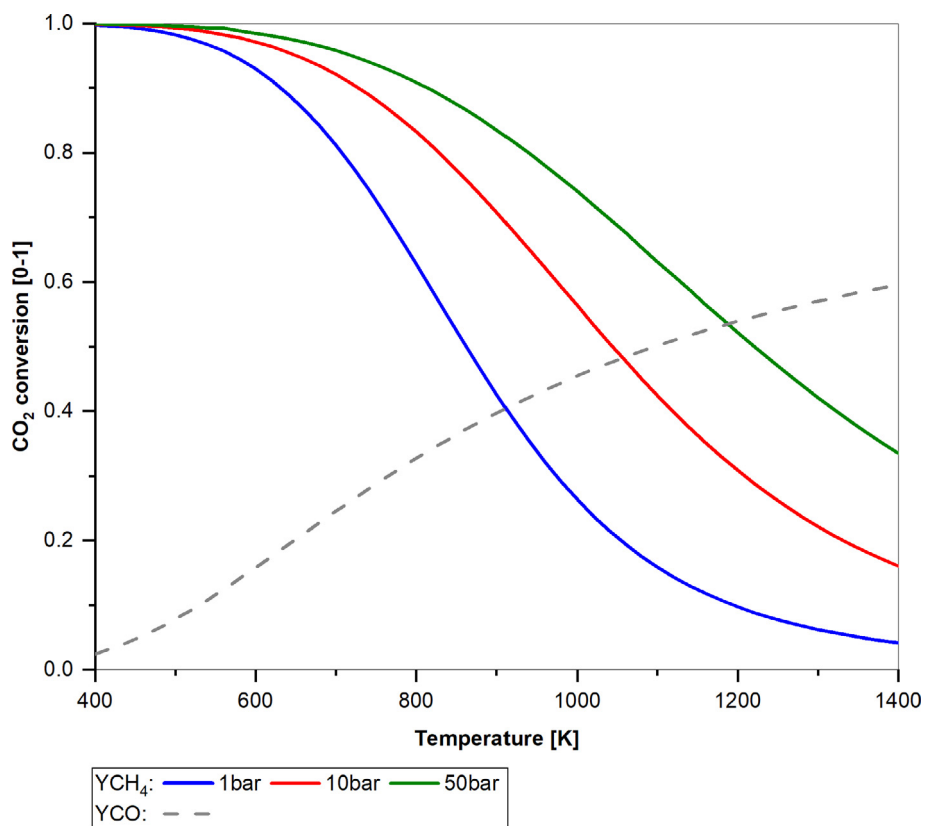


Fig. 1. Equilibrium conversion of CO₂ to CH₄ and CO for temperatures between 400 K and 1400 K and pressures from 1 bar to 50 bar. The exothermic Sabatier reaction is dependent on pressure. The endothermic RWGS reaction is independent of pressure. The reactions were calculated independent of each other.

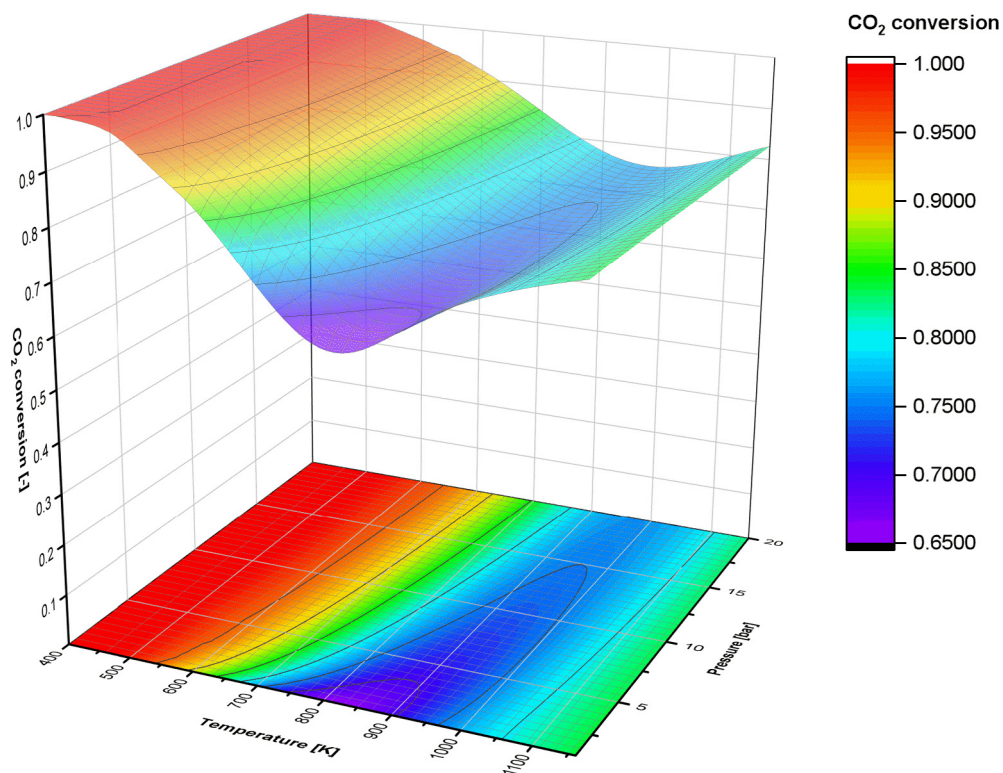
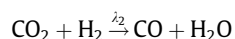
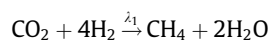


Fig. 2. Equilibrium conversion of CO₂ to CH₄ and CO as a function of temperature and pressure with the Sabatier and RWGS reaction occurring in parallel.

reaction temperatures since it is an endothermic reaction. This leads to an expected minimum in conversion in the temperature range of 800–900 K.

The thermodynamic analysis of the CO₂ hydrogenation reaction with the simultaneous formation of CH₄ and CO must be carried out using the extent of reaction method. For the system considered, two reactions are required to characterize the thermodynamic equilibrium.



where λ_1 and λ_2 are the fractions of reacted CO₂ for each reaction.

By doing the mass balance for both reactions and respecting the stoichiometry, the partial pressure of CO₂ after the reaction can be expressed as ($p_{\text{H}_2} = 4p_{\text{CO}_2}$)

$$p_{\text{CO}_2, \text{out}} = \frac{p_{\text{CO}_2, \text{in}} - \lambda_1 - \lambda_2}{5p_{\text{CO}_2, \text{in}} - 2\lambda_1} * p_{\text{tot}}$$

λ_1 and λ_2 are given by the equilibrium conversion for each reaction. The solution of the non-linear system:

$$\begin{cases} k_{\text{eq, Sabatier}} = \frac{p_{\text{CH}_4} * p_{\text{H}_2\text{O}}^2}{p_{\text{CO}_2} * p_{\text{H}_2}^4} \\ k_{\text{eq, RWGS}} = \frac{p_{\text{CO}} * p_{\text{H}_2\text{O}}}{p_{\text{CO}_2} * p_{\text{H}_2}} \end{cases}$$

gives the values of λ_1 and λ_2 as a function of temperature. On the basis of these values, the global conversion of CO₂ is determined. In general we, the CO₂ hydrogenation reaction to CH₄ is thermodynamically favored at low temperatures and therefore limited by reaction kinetics. At higher temperatures, the reaction becomes more selective to CO and is thermodynamically limited. Furthermore, the different influence of the two reactions is evident in the effect of pressure. While in the low temperature regime an increase of pressure causes a shift in the equilibrium concentration towards the products (and thus towards higher CO₂ conversion), at high temperature the pressure effect is not present. The origin of this difference is found in the different pressure dependence of the two reactions, due to the different stoichiometry (decrease in number of moles for methanation, constant number of moles for RWGS). With this calculation, the ideal working point for a desired product composition can be selected.

3.2. Reactivity investigation

3.2.1. CO₂ conversion and CH₄ yield over Fe, Co, Ni and Cu in comparison to Ru/Al₂O₃

The experimental results of the CO₂ hydrogenation reaction over Fe, Co, Ni and Cu are presented in this section. The results are compared to a 0.5 wt.% Ru/Al₂O₃ catalysts, since this is considered the state-of-the-art catalyst for the Sabatier reaction. The literature on Ru/Al₂O₃ catalysts in the CO₂ hydrogenation reaction goes back to 1973, when a catalytic performance study and a kinetic analysis of a 0.5 wt% Ru on Al₂O₃ was carried out by Lunde and Kester [18]. In that study, a maximum CO₂ conversion of 85% and an activation energy of 70.5 kJ/mol for the CO₂ conversion is reported. More recently the performance of 3% Ru/Al₂O₃ catalysts has been compared to a supported 20% Ni catalyst on Al₂O₃ [21]. An 86% methane yield with a selectivity close to 100% was found for the CO₂ hydrogenation reaction over the as prepared Ru based catalyst at 623 K while on the as prepared Ni based catalyst a 78% methane yield was measured with a 98% selectivity. Through pretreatment with reaction gas, they reported an increase in the methane yield to 96% on the Ru based catalyst. These results are in line with the reported 89% CO₂ conversion

with a methane selectivity close to 100% at 573 K and ambient pressure [22]. To ensure catalyst stability of the catalyst used in this work, a 24 h performance test was carried out with the Ru/Al₂O₃ catalyst (Sigma Aldrich 206199) at 655 K and ambient pressure after reducing the surface with H₂. No performance decline was detected after 24 h and the catalyst can be assumed to be stable which is in agreement with the findings in the literature [21]. This makes the Ru/Al₂O₃ catalyst an ideal reference for the present study.

In the following, the results of the CO₂ hydrogenation over Fe, Co, Ni, Cu and Ru/Al₂O₃ will be presented and discussed. Fig. 3 shows the CO₂ conversion (XCO₂) over the Ru/Al₂O₃ catalyst as a function of temperature at ambient pressure in relation to the equilibrium CO₂ conversion to CH₄ (YCH₄) and CO (YCO) and the equilibrium methane formation. The selectivity to methane is close to 100% at reaction temperatures up to 600 K. After the methane formation becomes thermodynamically limited at around 650 K, the selectivity towards CO, thermodynamically favored at higher reaction temperatures, drastically increases. From approximately 650 K on, the CO₂ conversion follows the shape of the calculated thermodynamic equilibrium. Prior to that temperature, the reaction is limited by kinetics and diffusion. The thermodynamically maximum conversion is not reached above 650 K since the reaction conditions are only quasi equilibrium conditions. The space velocity for the Ru/Al₂O₃ catalyst at a total reactant gas flow of 10 ml/min is 5305 h⁻¹. Therefore, the equilibrium is more closely approximated with a lower space velocity, which is equivalent to a longer residence time of the reactants in the reactor. To verify this assumption, the CO₂ conversion was measured at five different space velocities at 656 K with no He dilution (due to limitations in the possible MFC set points). A clear trend is visible (see Fig. 4), which shows that the equilibrium CO₂ conversion (88.2%) is closely approximated at a reactant gas flow of 2.5 ml/min (86.2%), while the CO₂ conversion decreases at a flow of 20 ml/min (74.7%) in comparison to the 10 ml/min reactant gas flow (76.9%). The space velocity of the Ru catalysts is larger than for the other metals, since the Ru is nanosized on the surface of the Al₂O₃ and therefore less catalyst mass is required to reach a comparable active surface area.

The pristine transition metals were measured in comparable conditions with approximately 1 g of catalyst grains mixed with the same weight of glass beads and at a space velocity of approximately 1000 h⁻¹. As summarized in Table 1, it was found that methane is the major product on Co and Ni, where the maximum CH₄ yield of 70.2% (at 661 K) on Co and 43.8% (at 786 K) on Ni is reached. On Fe, carbon monoxide is the main product and the maximum methane yield on Fe is 4.2% at 813 K. The methane yield goes through a maximum over Co, Ni and Ru/Al₂O₃, while the conversion keeps increasing on Fe until the maximum temperature measured (See Fig. 5). This indicates that on Fe the reaction does not reach the thermodynamic equilibrium within the temperature range considered. This is due to the lower reaction rate on Fe generated by limitation of various nature (e.g. lower activity of the catalyst and influence of diffusional limitations). The CO formation on the other hand is thermodynamically favored and the CO yield increases with temperature on all four metals. The highest CO yield on the active catalysts is measured on Fe with 22.4%, Ni 18.2% and Co with 6.9%. On Ru/Al₂O₃, the maximum CO yield is 26.2% at 813 K. C₂ + hydrocarbon products were only synthesized on Co, where a maximum C₂H₄ yield of 0.6% was measured at 528 K and a C₃H₆ yield of 0.2% yield at 516 K (Fig. 6). Anyhow, the C₂+ hydrocarbons formed contribute less than 1% to the overall CO₂ conversion. Cu as pristine metal showed no catalytic activity. We suppose that this is due to the low CO₂ absorption energy on Cu in comparison to Fe, Co and Ni [14].

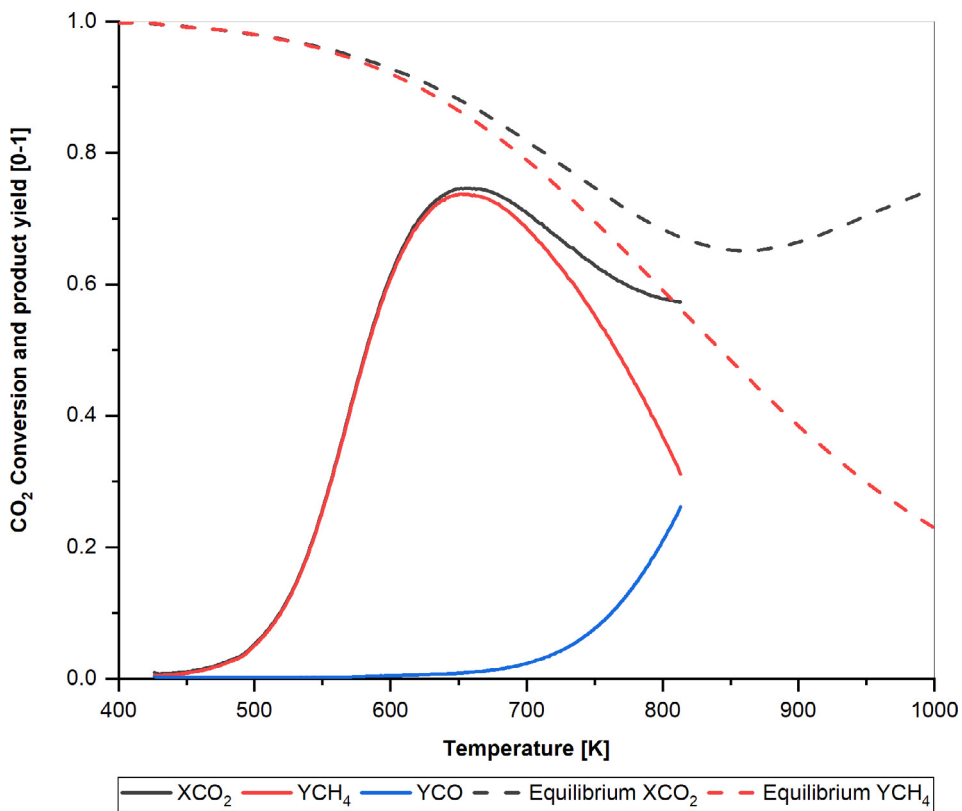


Fig. 3. CO₂ hydrogenation to CH₄ and CO over the Ru/Al₂O₃ catalyst in relation to the thermodynamic equilibria.

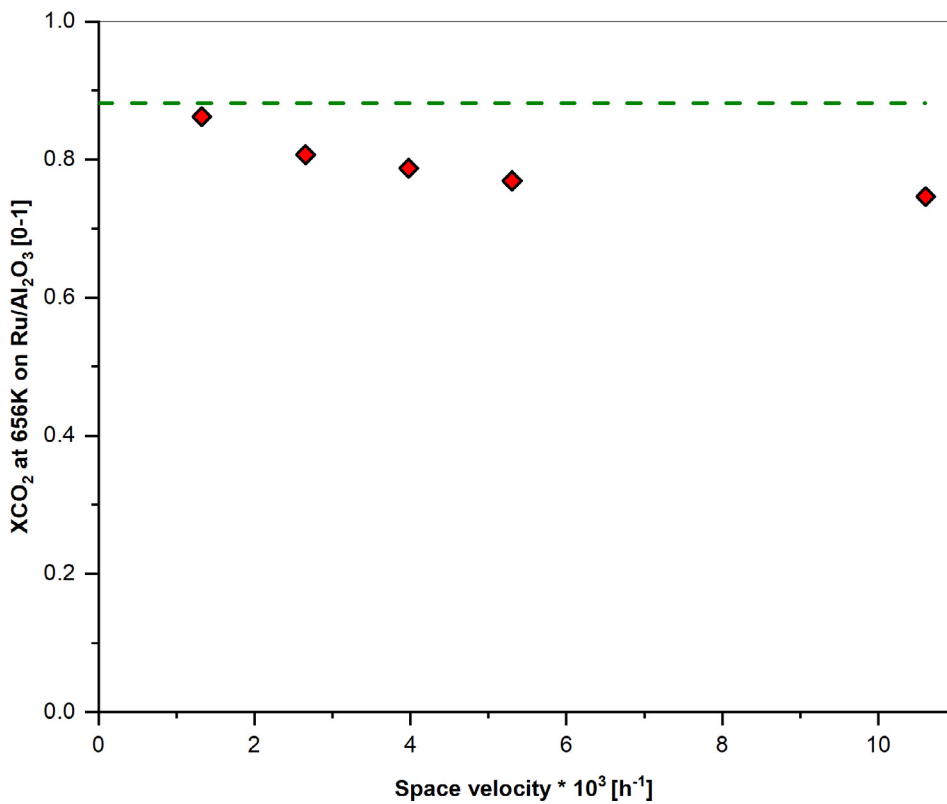
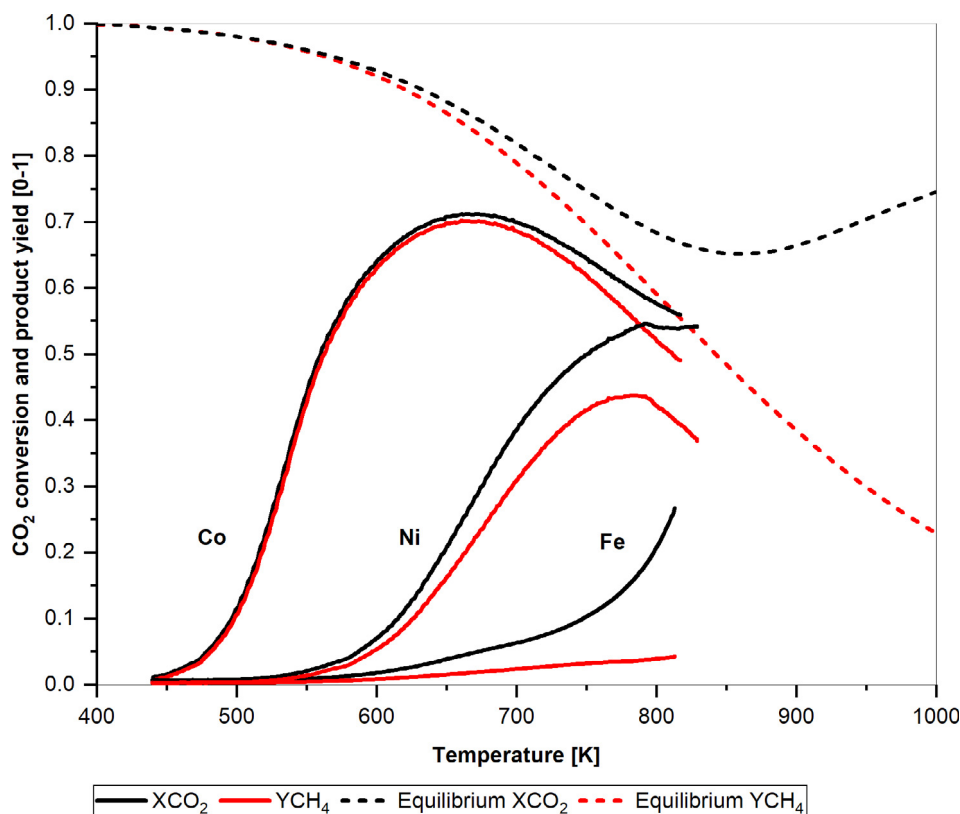


Fig. 4. Influence of the space velocity on the CO₂ conversion over Ru/Al₂O₃. The equilibrium is closer approached with decreasing space velocity.

Table 1Maximal CO₂ conversion, product yields and selectivity on each catalyst. ^{*}CO₂ conversion over Cu is similar to empty reactor.

Catalyst	Catalyst mass [g]	Space Velocity [h ⁻¹]	Max CO ₂ conversion		Max CH ₄ yield		Max CO yield		SCH ₄ [%] At XCO ₂ max	SCO [%]
			T [K]	XCO ₂ [%]	T [K]	Y [%]	T [K]	Y [%]		
Fe	1.0	1166	813	26.7	813	4.2	813	22.4	15.9	84.1
Co	1.0	965	661	71.2	661	70.2	817	6.9	98.6	1.4
Ni	1.0	956	792	54.7	786	43.8	829	18.2	79.9	20.1
Cu [*]	1.0	1200	805	58.9	653	1.2	805	58.0	1.6	98.4
Ru/Al ₂ O ₃	0.190	5305	652	74.7	652	73.4	813	26.2	98.8	1.2

**Fig. 5.** The CO₂ conversion and methane yield over Fe, Co and Ni. The difference between the CO₂ conversion (black) and methane yield (red) equals the CO yield.

3.3. Determination of the kinetic reaction parameters

The activation energy of the CO₂ hydrogenation been determined using the Arrhenius plot of the Turnover Frequency on Fe, Co, Ni and Ru/Al₂O₃.

3.3.1. Turnover frequency

The Turnover Frequency (TOF) was calculated to compare the CO₂ conversion over the different catalysts in relation to the active surface sites of each catalyst. The TOF of CO₂ over a catalyst relates the number of moles of CO₂ consumed in the reaction to the available active surface sites per time. The TOF is given by:

$$\text{TOF}_{\text{CO}_2} \left[\frac{1}{\text{s}} \right] = \frac{\sum \dot{n}_p}{n_{\text{cat}}} = \frac{n_{\text{CO}_2, \text{in}} \sum Y_p}{n_{\text{cat}}} \left[\frac{1}{\text{s}} \right]$$

where \dot{n}_p [mol/s] is the molar flow of the reaction products, n_{cat} [mol] the number of active surface sites, $n_{\text{CO}_2, \text{in}}$ [mol/s] the inflow of CO₂ and Y_p the yield of the reaction products. The number of active surface sites is calculated based on the assumption that the atoms are closest packed at the surface (face centered cubic –fcc and hexagonal close packing –hcp). The TOF is used for the further kinetic anal-

ysis of the reaction. The kinetic temperature range of the reaction is determined based on the linearity of the TOF in the Arrhenius plot.

3.3.2. Arrhenius plot

The Arrhenius equation expresses the relation between the reaction rate, the temperature and activation barrier. The Arrhenius equation is

$$k(T) = k_0 e^{\frac{E_a}{RT}}$$

where k_0 is the pre-exponential factor, E_a the activation energy, R the gas constant, T the reaction temperature, $k(T)$ is the rate constant in units of 1/s. The pre-exponential factor k_0 has the same unit. The exponential term is dimensionless. In the Arrhenius plot, where $\ln(k(T))$ is plotted versus $\frac{1}{T}$, the slope of the curve is $-\frac{E_a}{R}$ and the y-intercept is $\ln(k_0)$.

A major challenge is to identify the kinetically determined reaction temperature. In this range, the curve has a constant slope in the Arrhenius plot. This temperature range has to be identified in order to calculate the activation energy and determine the pre-exponential factor of the reaction. If the slope of the curve in the Arrhenius plot is plotted versus the inverse temperature, the kinetically determined reaction range is approximately constant. This

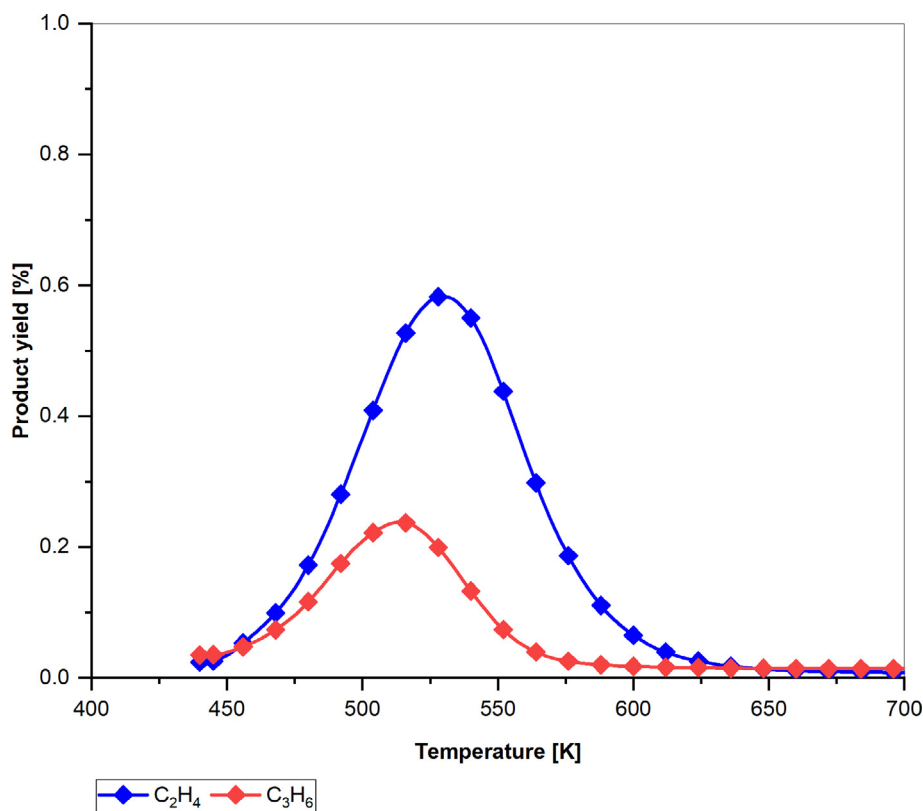


Fig. 6. C₂H₄ and C₃H₆ formation over Co as function of temperature.

temperature range was found to be about 30 K wide for all catalysts. It is 610–640 K for Fe, 480–510 K for Co, 600–630 K for Ni and 510–540 K for Ru/Al₂O₃ (see also Table 2). In these temperature ranges, k_0 and E_a were calculated based on a linear fit to the experimental data points. A very good data correlation was found for all catalysts with $R^2 \geq 0.999$. Fig. 7 shows the different reaction regions on the example of Co. Besides the kinetical limitations, also presumed diffusional and thermodynamic limitations are visible. Diffusional limitations occur if the reaction kinetics is faster than the molecular exchange between reactants and products on the catalyst surface. At higher reaction temperatures, the thermodynamic limitations become predominant. At low temperature (Fig. 7, region a), the conversion is low and thus the slope of the CO₂ curve is dominated by measurement noise due to the influence of the experimental error. Fig. 7, region b, shows the kinetically determined temperature range which is followed by region c), the diffusional- and thermodynamically limited temperature range.

It was found that the observed activation energies on Co, Ni and Ru/Al₂O₃ for these specific surface areas and reaction conditions are in close proximity with 77 kJ/mol for Co, 74 kJ/mol for Ni and 73 kJ/mol for Ru/Al₂O₃. With 50 kJ/mol, Fe has the lowest activation energy. Fig. 8 shows the Arrhenius plot for the kinetic temperature range with the linear fit and the experimental data points. Co, Ni and Ru/Al₂O₃ have a comparable slope since their observed

activation energies are close. The pre-exponential factor k_0 is calculated from the y- intercept of the Arrhenius plot. The results are shown in Fig. 8. It is found that Ru/Al₂O₃ has the highest k_0 (1.5E + 06), followed by Co (4.2E+05) and Ni (1.0E+05). Fe has a k_0 three orders of magnitudes lower than that of Co and Ni (See Fig. 9). A sensitivity analysis was carried out to investigate the influence of measurement error on the reaction temperature and the determined kinetic reaction range on the activation energy E_a and the frequency factor k_0 . With this analysis it was found that the influence on the activation energy of a temperature error of plus minus 10 K is marginal and results in a variation of one to three kJ/mol for the activation energies. The influence of a temperature on k_0 is more pronounced, since k_0 depends exponentially on the y-intercept in the Arrhenius plot, and therefore a small change in the slope of the curve has a significant influence on k_0 . However, the error on k_0 is within the order of magnitude of k_0 for all catalyst and therefore acceptable. The expected errors are indicated in Table 2.

3.3.3. Discussion of the Arrhenius parameters E_a and k_0 and catalyst activity

Comparing the activation energies determined in this study to the literature, one sees that the observed activation energy on the 0.5 wt% Ru/Al₂O₃ investigated in this work is in good agreement with the values reported [18,19,23,24]. The observed

Table 2
Kinetic temperature range for the determination of the activation energy and the determined activation energy E_a and the pre-exponential factor k_0 for the CO₂ conversion.

Catalyst	Fe	Co	Ni	Ru/Al ₂ O ₃
Kinetic temperature range [K]	610–640 (± 10)	480–510 (± 10)	600–630 (± 10)	510–540 (± 10)
Observed E_a [kJ/mol]	50 \pm 1	77 \pm 3	74 \pm 1	73 \pm 2
Observed k_0 [1/s]	(2.7 \pm 1)E+02	(4.2 \pm 0.6)E+05	(1 \pm 0.2)E+05	(1.5 \pm 1.5)E+06

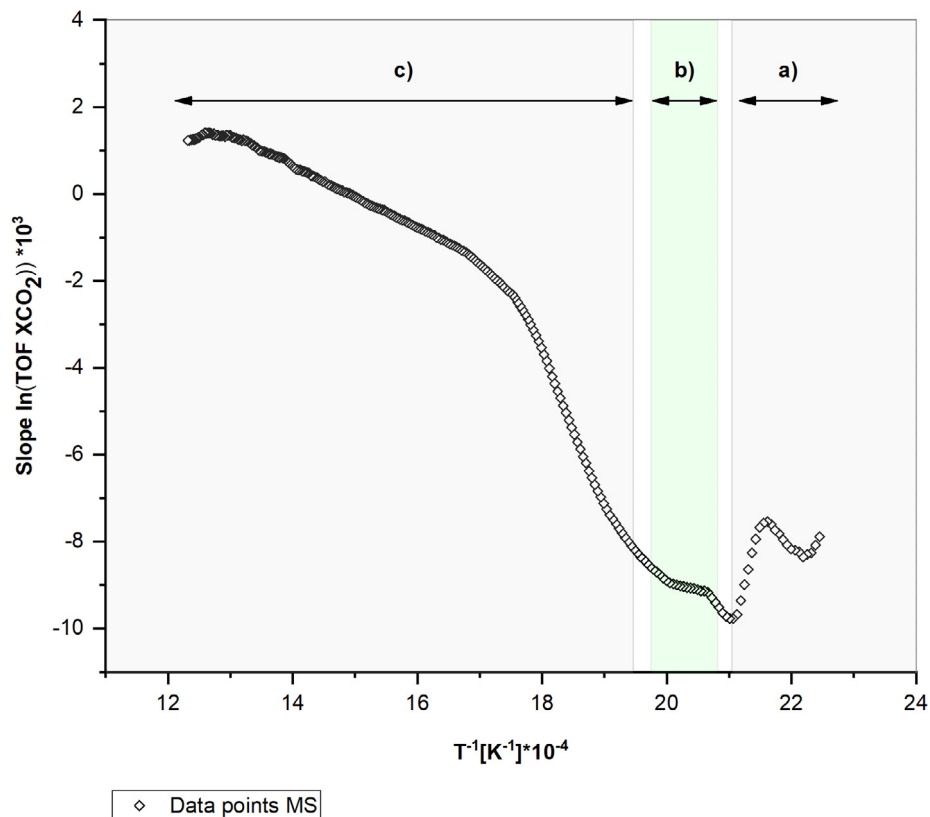


Fig. 7. Slope of the Arrhenius plot of the TOF of the CO₂ conversion over Co versus the inverse temperature. Temperature range (a) is the range of low conversion and therefore rich in noise. Section (b) is the approximately linear kinetically determined temperature range, followed by (c), the diffusional – and thermodynamically limited temperature range.

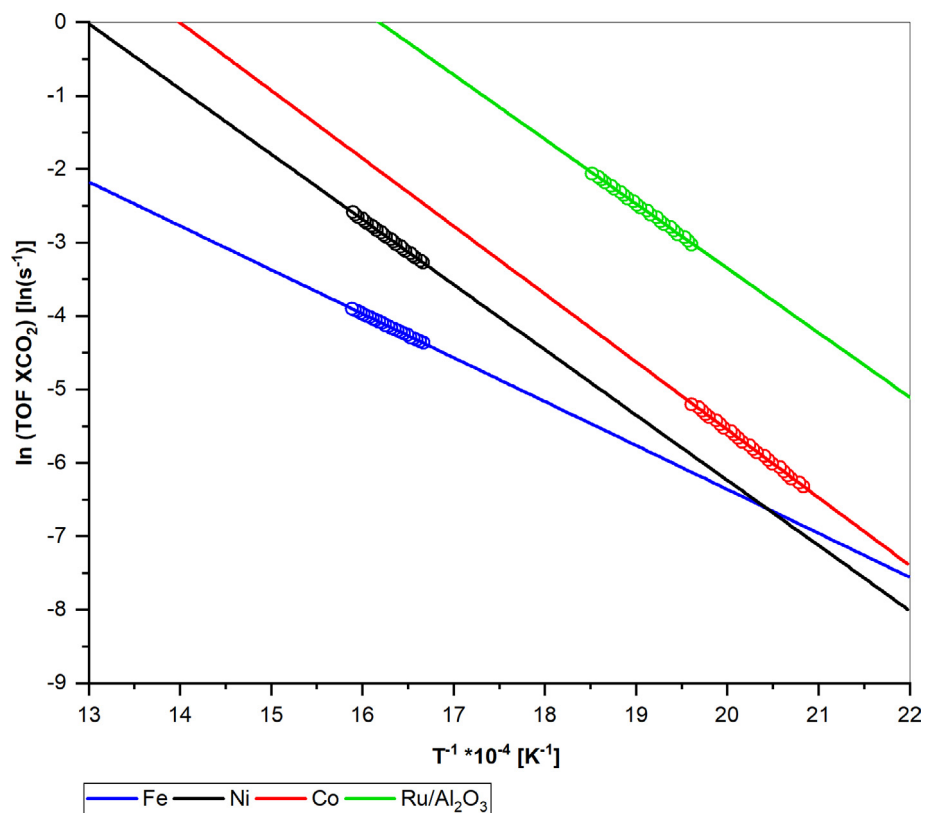


Fig. 8. Arrhenius plot with the experimental data of the kinetic temperature range for each catalyst with the extrapolated activation energy plot determined in the kinetic temperature range. The slope of the fitted linear curve is given by $-E_a/R$. The y intercept is $\ln(k_0)$.

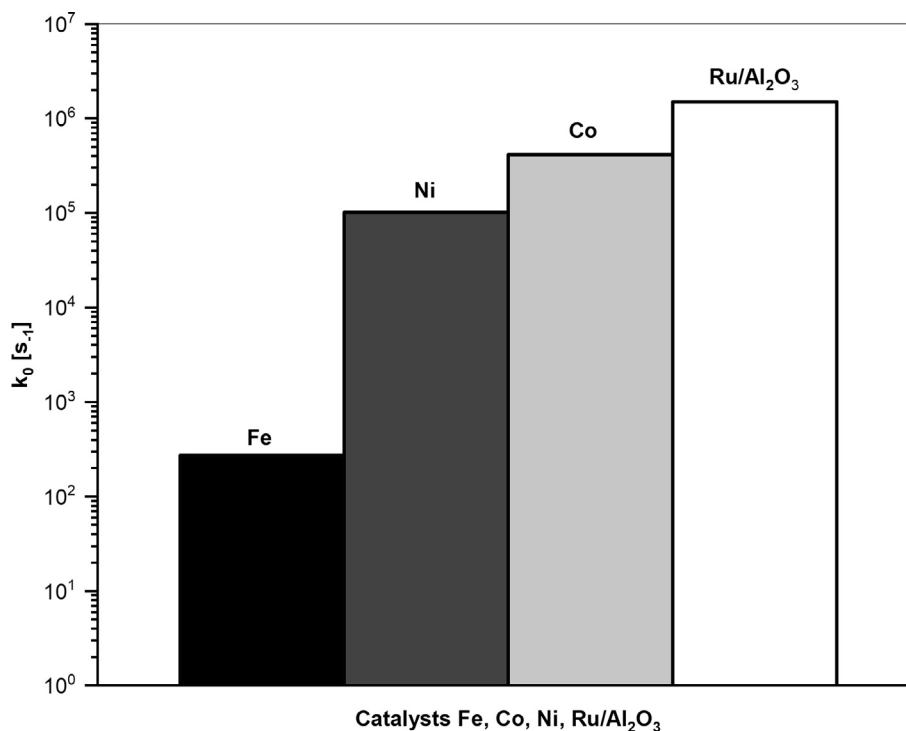


Fig. 9. Pre-exponential factors for CO₂ conversion on Fe, Ni Co and Al₂O₃ supported Ru.

activation energy of the CO₂ hydrogenation reaction over Fe determined in this work, where mainly the RWGS occurs, is also in line with literature values [25]. Anyways, literature is incomplete and a consistent determination of the activation energies of the CO₂ hydrogenation reaction on pristine Fe, Co, Ni and Cu is missing. Most of the activation energy values are reported for supported catalysts and it has been shown that the support has a large influence on the activation energy of the CO₂ hydrogenation over Ni supported on SiO₂, Al₂O₃ or TiO₂ [9]. The reported activation energies range from 69 kJ/mol for 3 wt% Ni on Al₂O₃ to 97 kJ/mol for an unsupported Ni catalyst. However, these values were not supported with an Arrhenius plot. In another study [19], the reported activation energies for 15 wt% Fe and Co supported on SiO₂, are 118 kJ/mol for Fe and 93 kJ/mol for Co at a reaction pressure of one bar.

For the Sabatier reaction, the rate constant $k(T)$ calculated from the Arrhenius equation is the apparent rate constant resulting from the difference between the direct and inverse reaction rates. Both of these reaction rates increase with increasing temperature, but the observed kinetic rate decreases with temperature due to the increase in the influence of the thermodynamic equilibrium. This results in an apparent increase of the frequency factor k_0 and in a decrease of the observed activation energy E_a . The reaction activation temperature depends on the reaction conditions. The activation energy and the frequency factor depend on the catalyst. If the catalyst is active for the CO₂ hydrogenation reaction, it provides a path with a lower activation energy compared to the uncatalyzed reaction, thus increasing the rate constant $k(T)$. A higher activation energy results in a greater dependence of the rate constant on the temperature increase. Therefore, the slope of the CO₂ conversion curve as a function of temperature is larger for a higher activation energy. This is in accordance with the experimental findings, where the conversion increases more rapidly on Co, Ni and Ru/Al₂O₃ in comparison to Fe. Furthermore, the similar values of the activation energy over Co, Ni and Ru/Al₂O₃ suggest the presence of a similar mechanism for the reaction on the three catalysts.

On the other hand, k_0 expresses the rate constant for an infinite temperature or a reaction without activation (ergo where every reactant collision results in the formation of a product). In practice, k_0 influences the activation temperature of the catalyzed reaction. E.g., if two catalysts with similar activation energies are compared, the catalyst that has a larger k_0 activates at a lower temperature. This is observed for Co and Ni, where Ni activates more than 100 K later than Co. However, for the case of Co and Ni, the difference in k_0 (3E+05) is not sufficient to justify this difference of activation temperature. The calculated activation temperature difference based on the Arrhenius parameters is around 20 K. The later activation can be explained by the influence of mass transfer limitations at higher temperatures. For 1 g of Co and Ni, there are approximately ten times more surface sites available on Co due to the larger specific surface area (Table 2, SI). Therefore, the space velocity of 956 h⁻¹, which is globally the same for Co and Ni, is approximately ten times higher than the available surface sites for Ni, which then results in the later reaction activation of Ni. This interpretation is supported by an experiment, where the activity of 0.1 g of Co was compared to 1 g of Ni. The 0.1 g of Co, which has approximately the same number of available surface sites as 1 g of Ni, activated at a higher temperature than 1 g of Co, close to the activation temperature of 1 g Ni. The thermodynamic influence on the reaction is stronger at elevated temperatures. Therefore, the later activation of the catalysts results in a limited maximal conversion due to the thermodynamic influence on the reaction. Furthermore, the concentration of the gases has an influence on the observed activation energy. In fact, the absence of He as a carrier gas generates an increase in the observed activation energy to 96 kJ/mol for Co, 91 kJ/mol for Ru/Al₂O₃ and 78 kJ/mol for Ni. This is due to the stronger influence of the reaction hotspot of the exothermic methanation reaction in the non-diluted reaction gas. The effect is less pronounced with Ni, where the observed activation energy increases by only 4 kJ/mol since the influence of the hot-spot is weaker at the higher reaction temperature of Ni. The results of the experiments in the absence of helium shows how the

temperature management and consequently the determination of the activation energy is a challenging task in a highly exothermal reaction as the CO₂ methanation. He as a diluting agent is used to enable a better temperature control by reducing the reaction hotspot.

These findings lead to the interpretation, that Co, Ni and Ru/Al₂O₃ have comparable abilities to catalyze the CO₂ hydrogenation reaction, while Fe has only little activity in the Sabatier reaction and Cu exhibits no catalytic activity in the CO₂ hydrogenation reaction. The differences between the investigated systems mostly comes from the availability of surface sites, the actual space velocity with respect to the surface sites and the diffusional limitations based on the shape and size distribution of the catalyst.

4. Conclusion

In this study we have investigated the catalytic activity of the pristine transition metal catalysts Fe, Co, Ni, Cu along with the reference system 0.5 wt% Ru supported on Al₂O₃. The experiments were carried out in comparable conditions for all catalysts and were framed with a thermodynamic reaction analysis.

It was found that Co and Ni are the most active catalysts in the CO₂ hydrogenation reaction among the investigated pristine metals and they exhibit a high selectivity to methane. Fe on the other hand was mostly active in the CO formation and therefore in the reverse water gas shift reaction. Cu showed no catalytic activity as a pristine metal.

The kinetically determined reaction range was identified based on a quantitative gas analysis method by means of mass spectrometry. With this method, rapid gas sampling can be achieved, and the kinetic reaction range can be identified with high accuracy due to the high density of data-points.

The observed activation energies of the CO₂ hydrogenation reaction were found to be comparable for Co, Ni and Ru/Al₂O₃ in these reaction conditions, suggesting a similar reaction path. A different reaction path presumably occurs for Fe, since both its activation energy and the frequency factor were significantly lower in comparison to the other active catalysts. The space velocity and the availability of active surface sites have a critical influence on the activation temperature of the catalysts, and due to thermodynamic limitations at higher reaction temperatures, on the maximum CO₂ conversion.

With this work we contribute to the better fundamental understanding of the industrially significant catalyst building blocks Fe, Co, Ni and Cu. This study sets the basis for further investigations of the reaction kinetics.

Acknowledgement

Financial support by the Swiss National Science Foundation: Project “Investigation and modeling of new CO₂ adsorption materials and their interaction with hydrogen” Verfügung 200021_163010/1 and the SCCER Heat & Electricity Storage (innosuisse) are acknowledged. Furthermore, Dr. Emad Oveisi is

acknowledged for his support in performing the SEM image measurements.

References

- [1] M. Armand, Building better batteries, *Nature* 451 (2008) 652–657.
- [2] A. Züttel et al., Storage of renewable energy by reduction of CO₂ with hydrogen, *Chim. Int. J. Chem.* 69 (2015) 264–268.
- [3] C. Graves, S.D. Ebbesen, M. Mogensen, K.S. Lackner, Sustainable hydrocarbon fuels by recycling CO₂ and H₂O with renewable or nuclear energy, *Renew. Sustain. Energy Rev.* 15 (2011) 1–23.
- [4] M.D. Porosoff, B. Yan, J.G. Chen, Catalytic reduction of CO₂ by H₂ for synthesis of CO, methanol and hydrocarbons: challenges and opportunities, *Energy Environ. Sci.* 9 (2016) 62–73.
- [5] Gerard P. Van Der Laan, A.A.C.M. Beenackers, Kinetics and selectivity of the Fischer Tropsch synthesis: a literature review, *Catal. Rev. – Sci. Eng.* 41 (1999) 255–318.
- [6] W. Wang, S. Wang, X. Ma, J. Gong, Recent advances in catalytic hydrogenation of carbon dioxide, *Chem. Soc. Rev.* 40 (2011) 3703–3727.
- [7] S. Kattel, P. Liu, J.G. Chen, Tuning selectivity of CO₂ hydrogenation reactions at the metal/oxide interface, *J. Am. Chem. Soc.* 139 (2017) 9739–9754.
- [8] E.D. Goodman, J.A. Schwalbe, M. Cargnello, Mechanistic understanding and the rational design of sinter-resistant heterogeneous catalysts, *ACS Catal.* 7 (2017) 7156–7173.
- [9] C.K. Vance, C.H. Bartholomew, Hydrogenation of carbon dioxide on group viii metals, *Appl. Catal.* 7 (1983) 169–177.
- [10] K. Larmier et al., CO₂-to-methanol hydrogenation on zirconia-supported copper nanoparticles: reaction intermediates and the role of the metal-support interface, *Angew. Chem. – Int. Ed.* 56 (2017) 2318–2323.
- [11] H.J. Freund, M.W. Roberts, Surface chemistry of carbon dioxide, *Surf. Sci. Rep.* 25 (1996) 225–273.
- [12] F. Solymosi, The bonding, structure and reactions of CO₂ adsorbed on clean and promoted metal surfaces, *J. Mol. Catal.* 65 (1991) 337–358.
- [13] J.K. Nørskov et al., The nature of the active site in heterogeneous metal catalysis, *Chem. Soc. Rev.* 37 (2008) 2163–2171.
- [14] C. Liu, T.R. Cundari, A.K. Wilson, CO₂ reduction on transition metal (Fe, Co, Ni, and Cu) surfaces: In comparison with homogeneous catalysis, *J. Phys. Chem. C* 116 (2012) 5681–5688.
- [15] S.-G. Wang et al., Factors controlling the interaction of CO₂ with transition metal surfaces, *J. Phys. Chem. C* 111 (2007) 16934–16940.
- [16] R. van Santen, J. Markvoort, I.W. Filot, M.M. Ghouri, E.J.M. Hensen, Mechanism and microkinetics of the Fischer-Tropsch reaction, *Phys. Chem. Chem. Phys.* 15 (2013) 17038–17063.
- [17] R.A. Van Santen, I.M. Ciobică, E. Van Steen, M.M. Ghouri, Mechanistic issues in Fischer-Tropsch catalysis, *Adv. Catal.* 54 (2011) 127–187.
- [18] P. Lunde, F.K. Kester, Rates of methane formation from carbon dioxide and hydrogen over a ruthenium catalyst, *J. Catal.* 30 (1973) 423–429.
- [19] G.D. Weatherbee, C.H. Bartholomew, Hydrogenation of CO₂ on group VIII metals. IV. Specific activities and selectivities of silica-supported Co, Fe, and Ru, *J. Catal.* 87 (1984) 352–362.
- [20] G.D. Weatherbee, C.H. Bartholomew, Hydrogenation of CO₂ on group VIII metals. II. Kinetics and mechanism of CO₂ hydrogenation on nickel, *J. Catal.* 77 (1982) 460–472.
- [21] G. Garbarino, D. Bellotti, P. Riani, L. Magistri, G. Busca, Methanation of carbon dioxide on Ru/Al₂O₃ and Ni/Al₂O₃ catalysts at atmospheric pressure: catalysts activation, behaviour and stability, *Int. J. Hydrogen Energy* 40 (2015) 9171–9182.
- [22] M. Schoder, U. Armbruster, A. Martin, Heterogen katalysierte Hydrierung von Kohlendioxid zu Methan unter erhöhten Drucken, *Chem. – Ing. – Tech.* 85 (2013) 344–352.
- [23] X. Wang, Y. Hong, H. Shi, J. Szanyi, Kinetic modeling and transient DRIFTS-MS studies of CO₂ methanation over Ru/Al₂O₃ catalysts, *J. Catal.* 343 (2016) 185–195.
- [24] L. Falbo et al., Kinetics of CO₂ methanation on a Ru-based catalyst at process conditions relevant for Power-to-Gas applications, *Appl. Catal. B Environ.* 225 (2018) 354–363.
- [25] Jason A. Loiland, Matthew J. Wulfers, Nebojsa S. Marinkovic, F.R. Lobo, Fe-γ-Al₂O₃ and Fe-K-γ-Al₂O₃ as reverse water gas shift catalysts, *Catal. Sci. Technol.* 6 (2016) 5267–5279.